Journal of Cleaner Production 451 (2024) 141810

Contents lists available at ScienceDirect

Journal of Cleaner Production

journal homepage: www.elsevier.com/locate/jclepro

Polyhydroxyalkanoates production from a waste-derived feedstock driven by the reactor operating conditions: The role of biomass microbiome and its reactivation capacity

Eliana C. Guarda [a,b], Catarina L. Amorim [c], Gabriele Pasculli [a,b], Paula M.L. Castro [c], Claudia F. Galinha [d], Anouk F. Duque [a,b,*], Maria A.M. Reis [a,b]

[a] Laboratory i4HB - Institute for Health and Bioeconomy, NOVA School of Science and Technology, Universidade NOVA de Lisboa, 2829-516, Caparica, Portugal
[b] UCIBIO – Applied Molecular Biosciences Unit, Department of Chemistry, NOVA School of Science and Technology, Universidade NOVA de Lisboa, 2829-516, Caparica, Portugal
[c] Universidade Católica Portuguesa, CBQF – Centro de Biotecnologia e Química Fina – Laboratório Associado, Escola Superior de Biotecnologia, 4169-005, Porto, Portugal
[d] LAQV-REQUIMTE, Chemistry Department, NOVA School of Science and Technology, Universidade NOVA de Lisboa, 2819-516, Caparica, Portugal

ARTICLE INFO

Handling Editor: Jian Zuo

Keywords:
Mixed microbial cultures (MMC)
Polyhydroxyalkanoates
Microbiome
Biomass reactivation
Productivity

ABSTRACT

In the last years, the production of plastics at large-scale has been an issue of great concern due to their environmental and health impacts. Biobased and biodegradable plastics, such as polyhydroxyalkanoates (PHA), have emerged as a possible more ecological and sustainable alternative to those conventional plastics. PHA can be produced by mixed microbial cultures (MMC) from waste-based feedstocks. This work aimed to maximize the PHA production from fermented brewer's spent grain by selecting an efficient PHA-accumulating MMC, applying different organic loading rates (OLR, 45 or 60 $C mmol_{FP}/(L.d)$) and sludge retention times (SRT, 4 or 2 days). Additionally, the biomass reactivation capacity after storage was evaluated.

The global PHA productivity depends on the operating conditions, achieving its maximum (3.55 ± 0.8 $g_{PHA}/(L.d)$) at the highest OLR and SRT tested. After storage, the global PHA productivity was similar to the one achieved before the starvation period.

Depending on the operating conditions, the microbiome has its own bacterial composition signature containing various PHA-producers genera (e.g., *Acidovorax*, *Amaricoccus*, *Brevundimonas*, *Leucobacter*, *Leadbetterella* and *Thauera*) that persisted over time, albeit at different relative abundancies.

A comprehensive overview of PHA production with data on system performance and microbiome is presented, which thereby can further contribute to the upscale of such valorisation processes.

1. Introduction

Petrochemical plastics have been largely produced since their discovery in the 19th century, mainly due to their interesting and easily manipulated properties and use in a broad range of applications. However, as they are non-biodegradable materials, their accumulation in the environment can pose threats to the ecosystems and human life (United Nations Environment Programme, 2024). Thus, the need for more sustainable plastic materials led to a huge demand for alternative options such as bioplastics. In the coming years, the rising trend of bioplastics production is expected to continue, with an estimated production increase of 3.9 million tones (Mt) from 2023 to 2027 (European Bioplastics, 2022). Within the bioplastics group, the ones that are biobased and biodegradable, such as polyhydroxyalkanoates (PHA), have shown a lower environmental footprint of production than the traditional plastics (Gurieff and Lant, 2007). In fact, like the global bioplastics production, the PHA market size has also a rising trend with around 98 million USD projected for 2028 (Statistica, 2024).

PHA are biodegradable and biocompatible polymers produced by pure or mixed microbial cultures (MMC) either using synthetic and pure carbon sources or low-cost/waste feedstocks (Reis et al., 2011). Up to now, the major drawback of the PHA production processes is its high production costs (5.0 EUR/kg for PHA vs. 0.8–1.5 EUR/kg for oil-based

* Corresponding author. UCIBIO – Applied Molecular Biosciences Unit, Department of Chemistry, NOVA School of Science and Technology, Universidade NOVA de Lisboa, 2829-516 Caparica, Portugal.
E-mail address: af.duque@fct.unl.pt (A.F. Duque).

https://doi.org/10.1016/j.jclepro.2024.141810
Received 13 November 2023; Received in revised form 22 February 2024; Accepted 15 March 2024
Available online 16 March 2024

Abbreviations

3HB	3-hydroxybutyrate
3HHx	3-hydroxyhexanoate
3HV	3-hydroxyvalerate
3H2MV	3-hydroxy-2-methylvalerate
DO	Dissolved oxygen
EtOH	Ethanol
fBSG	Fermented brewer's spent grain
F/f	Feast to famine ratio
FP	Fermentation products
GC	Gas chromatography
HAc	Acetic acid
HBut	Butyric acid
HCap	Caproic acid
HIsoBut	Isobutyric acid
HIsoVal	Isovaleric acid
HPLC	High performance liquid chromatography
HProp	Propionic acid
HRT	Hydraulic retention time
HVal	Valeric acid
MMC	Mixed microbial cultures
OLR	Organic loading rate
PHA	Polyhydroxyalkanoates
$-q_{FP}$	Specific fermentation products consumption rate
$-q_{FPmax}$	Maximum specific fermentation products consumption rate
q_{PHA}	Specific PHA storage rate
q_{PHAmax}	Maximum specific PHA storage rate
r_{PHA}	PHA volumetric productivity
SBR	Sequencing batch reactor
SRT	Sludge retention time
TS	Dry weight after lyophilization
TSS	Total suspended solids
VSS	Volatile suspended solids
X_A	Active biomass
XPR	Biomass volumetric productivity
$Y_{PHA/FP}$	PHA storage yield on FP consumed

plastics) (Crutchik et al., 2020; Saavedra del Oso et al., 2021). Aiming at decreasing the operational costs of PHA production processes, the use of MMC and low-cost/waste feedstocks is a promising strategy (Carvalheira et al., 2022; Duque et al., 2014; Matos et al., 2021a; Sabapathy et al., 2020). The PHA production using MMC comprises three stages: (1) conversion of the organic matter through acidogenic fermentation into a fermentation products (FP) mixture, composed by carboxylic acids, which are the PHA precursors; (2) selection of an aerobic microbial community enriched in PHA-storing organisms; and (3) PHA accumulation up to the maximum culture capacity, by using the selected culture (stage 2) and the FP (stage 1) (Reis et al., 2011). The success of the entire PHA production process by MMC is not dependent solely on the last stage of PHA accumulation. Indeed, it can be compromised if there is not a good selection of PHA-storers. A high and stable PHA storage ability and a high biomass growth rate are desired to improve the global PHA productivity (Reis et al., 2011).

Aiming at increasing the process productivity, some operating parameters can be manipulated over the culture selection stage. One of the key factors is the organic loading rate (OLR) as higher values often allow to work with a lower selection reactor volume while achieving higher selected biomass concentrations, which might result in higher PHA production levels (Carvalheira et al., 2022; Cruz et al., 2022). Additionally, the sludge retention time (SRT), an indicator of the microorganisms' age, also affects the process productivity by impacting the competition between the PHA storage and growth metabolic pathways. Generally, at lower SRT, microorganisms mostly use carbon to grow instead of storing PHA, resulting in a selection of populations with more ability to grow (Reis et al., 2011). Additionally, the reactor start-up for culture selection is often long and challenging, often hindering this process application. Therefore, the use of stored pre-selected cultures (e.g. purged biomass from reactors) could be an interesting approach. However, if a selected culture is stored and, thus, subjected to a starvation period, its microbial composition may change. Thus, the impact of different operating conditions and storage periods on the biomass behavior and composition, especially in terms of PHA-storers abundance, should be further investigated.

In this study, the selection of an efficient PHA-accumulating MMC was evaluated using fermented brewer's spent grain (fBSG) as feedstock. The impact of different operating parameters, namely the organic loading rate (OLR) and sludge retention time (SRT), and the effect of a starvation period on the culture performance and its PHA production ability after resuming operation were investigated and related to changes in the culture microbiome composition. The biomass reactivation performance after a starvation period allows to evaluate the impact of a long and sudden industrial plant shut down on the culture performance during the reactor restart.

2. Materials and methods

2.1. Feedstock

A fermented brewers' spent grain produced in a previous work was used as feedstock (Guarda et al., 2023). The fBSG was composed by a mixture of (% Cmol basis): acetic acid (39.8 ± 5.3%), propionic acid (2.3 ± 1.9%), isobutyric acid (4.9 ± 1.4%), butyric acid (32.3 ± 2.1%), isovaleric acid (3.4 ± 0.7%), valeric acid (1.5 ± 0.8%), caproic acid (14.2 ± 5.2%) and ethanol (1.5 ± 1.1%). The fBSG had a C:N:P ratio of 100:9:0.1 (mol basis), being rich in ammonia (NH_4^+) but with a limited phosphate content (PO_4^{3-}).

2.2. Reactor set-up for culture selection

A sequencing batch reactor (SBR) of 2 L working volume was inoculated with activated sludge from a wastewater treatment plant (Mutela in Almada, Portugal) and fed with fBSG. The reactor was operated under 12 h cycles of feast and famine periods comprising: 11.25 h of reaction (aeration and stirring), 40 min of settling (without aeration and stirring) and 5 min of reactor withdrawn (1 L). During the first 5 min of each new cycle, 1 L of fresh media (fBSG and a mineral solution as described by Wang et al. (2017)) was added. After 2 h, a phosphate-rich solution (KH_2PO_4) was added to the reactor in order to assure a C:N:P ratio of 100:9:1 (mol basis). The reactor was operated at room temperature (20–25 °C) and the pH was controlled between 7.5 and 8.5 through the automatic addition of 0.5 M HCl or 1 M NaOH solutions. The air was supplied through a disperser and the dissolved oxygen (DO) levels were kept above 20% by adjusting the air flow rate (2–4 L/min) and the stirring (100–200 rpm), using a flat blade turbine type stirrer. The length of the feast and famine periods of the SBR cycles was monitored through the continuous acquisition of both pH and DO data.

The reactor operation lasted for 6 months, divided into 4 phases, according to Table 1. A starvation period of 3 months was imposed to the system after phase III, mimicking the shutdown period of an industrial facility, during which the biomass was stored at 4 °C. The reactor was later reactivated on phase IV using the stored biomass, and was operated under the same conditions of phase II for 1 month. Throughout operation, once a pseudo-steady state was achieved for each phase, the SBR

Table 1
The SBR biomass performance at pseudo-steady state for each operating phase. Values presented are means ± standard deviations.

	Phase I	Phase II	Phase III		Phase IV
Operation days (days)	0 to 70	71 to 119	120 to 170		259 to 288
Monitoring cycles (number)	4	4	5		2
SRT (days)	4.3 ± 0.1	3.8 ± 0.1	2.0 ± 0.0		4.2 ± 0.2
HRT (days)	1.1 ± 0.02	1.1 ± 0.02	1.1 ± 0.06		1.0 ± 0.01
F/f ratio (h/h)	0.08 ± 0.02	0.07 ± 0.01	0.08 ± 0.01		0.05 ± 0.01
OLR ($Cmmol_{FP}$/(L.d))	43.0 ± 1.5	60.8 ± 6.0	64.8 ± 5.3		60.0 ± 7.6
-q_{FP} ($Cmmol_{FP}$/($Cmmol_{XA}$.h))	0.42 ± 0.10	0.46 ± 0.08	0.53 ± 0.09		0.33 ± 0.01
q_{PHA} ($Cmmol_{PHA}$/($Cmmol_{XA}$.h))	0.32 ± 0.09	0.39 ± 0.10	0.45 ± 0.06		0.27 ± 0.01
$Y_{PHA/FP}$ ($Cmmol_{PHA}$/$Cmmol_{FP}$)	0.78 ± 0.05	0.83 ± 0.07	0.84 ± 0.07	Starvation period	0.83 ± 0.004
PHA_{max_Feast} (% g_{PHA}/g_{TS})	19.2 ± 2.9	18.4 ± 2.1	24.5 ± 3.8		14.8 ± 1.7
(g_{PHA}/L)	0.70 ± 0.2	1.12 ± 0.2	1.02 ± 0.2		0.95 ± 0.1
r_{PHA} (g_{PHA}/(L.d))	1.03 ± 0.4	2.40 ± 0.5	1.26 ± 0.2		1.48 ± 0.3
X_A (g_{XA}/L)	2.4 ± 0.9	4.1 ± 0.5	2.4 ± 0.1		4.4 ± 0.7
XPR (g_{XA}/(L.d))	0.57 ± 0.20	1.09 ± 0.11	1.24 ± 0.05		0.98 ± 0.14
Polymer composition (% Cmol)					
3HB	78 ± 2	75 ± 1	79 ± 4		78 ± 1
3HV	12 ± 1	11 ± 1	10 ± 3		13 ± 3
3H2MV	3 ± 2	5 ± 1	3 ± 1		4 ± 1
3HHx	5 ± 5	9 ± 0.5	8 ± 1		5 ± 3

performance was monitored by analyzing the PHA, FP, NH_4^+, PO_4^{3-} and total and volatile suspended solids (TSS and VSS) contents. Additionally, biomass samples were collected for DNA analysis.

2.3. PHA accumulations assays experimental set-up

In each operating phase, when the SBR reached a pseudo-steady state, the biomass was used to perform PHA accumulations assays. The assays were carried out in reactors of 1 L working volume (New Brunswick™ BioFlo®/CelliGen® 115 system) in fed-batch mode. The assays were performed at room temperature using 500 mL of the enriched biomass collected from the SBR at the end of the famine period and fBSG as feedstock. The air flow rate was controlled between 2.5 and 5 L/min and the stirring at 200 rpm to assure DO levels above 20%. The pH was controlled within the range of 7.5–8.5 by the automatic addition of 0.5 M HCl or 1 M NaOH solutions. The PHA accumulation assays were performed using a pulse-wise feeding strategy controlled by the DO. The sudden DO increase corresponded to the end of a pulse, then a new pulse of fBSG was added to the reactor. Each assay was carried out until the metabolic activity substantially slowed down (no DO response observed). Samples were collected over the accumulation assays for the same parameters as for the SBR operation (excluding samples for DNA analysis).

2.4. Analytical procedures

Throughout the SBR cycles and PHA accumulation assays, samples from the mixed liquor inside the reactor were collected and centrifuged (11000 ×*g*, 2 min). The resulting supernatants were filtered (0.2 μm membrane filters) and stored at −20 °C while the pellets were lyophilized. TSS and VSS were quantified according to the standard methods (Apha, 2012). The FP quantification was performed by high performance liquid chromatography as described by Duque et al. (2014). NH_4^+ and PO_4^{3-} contents were determined by a colorimetric method implemented in a continuous flow analyzer (Skalar San ++, Skalar Analytical, The Netherlands). The PHA quantification and composition were determined through gas chromatography as described by Pereira et al. (2023) but with some changes. In the present study, the lyophilized pellets (1–3 mg) were hydrolyzed at 100 °C for 3.5 h in sealed tubes, using 1 mL of 20% (v/v) sulfuric acid in methanol and 1 mL of chloroform containing heptadecanoate (HD) as internal standard (0.5 g/L). Furthermore, 3-hydroxybutyrate (3HB) and 3-hydroxyvalerate (3HV) monomers were quantified using a commercial PHBV (Sigma-Aldrich, 88 mol% 3HB, 12 mol% 3HV) co-polymer as standard.

2-Hydroxyhexanoic was used as standard to quantify the 3-hydroxy-2--methylvalerate (3H2MV) monomers as previously described by Oehmen et al. (2005), where it was reported that the relative response factor between 2-hydroxyhexanoic acid and 3H2MV is similar in the GC quantification, as these two molecules are isomers of each other. Methyl-3-hydroxyhexanoate was used as standard to quantify the 3-hydroxyhexanoate (3HHx) monomers.

2.5. Performance parameters calculations

The Feast to famine ratio (F/f in h/h) was calculated by dividing the length (h) of the feast (F) period by the length of the famine (f) period of the SBR cycles. The PHA content in the biomass was determined in terms of percentage of total solids (TS) (in % g_{PHA}/g_{TS}), where the g_{PHA} was calculated by summing all the monomers (3HB, 3HV, 3H2MV, 3HHx) contents and g_{TS} is the weight after lyophilization. Bulk PHA and active biomass (X_A) concentrations (in g_{PHA}/L and g_{XA}/L, respectively) and the specific FP consumption and PHA production rates ($-q_{FP}$ in $Cmmol_{FP}/(Cmmol_{XA}.h)$ and q_{PHA} in $Cmmol_{PHA}/(Cmmol_{XA}.h)$, respectively) were calculated as described by Rangel et al. (2023). The PHA storage yield on FP consumed ($Y_{PHA/FP}$ in $Cmmol_{PHA}/Cmmol_{FP}$) was assessed by dividing the q_{PHA} by the $-q_{FP}$. Biomass (XPR in $g_{XA}/(L.d)$) and PHA (r_{PHA} in $g_{PHA}/(L.d)$) volumetric productivities were determined as described by Matos et al. (2021b) and Carvalheira et al. (2022), respectively.

For the PHA accumulation assays, the maximum specific rates and yields for each pulse were calculated as described for the SBR operation. The average values of each parameter for the two first pulses were considered to assess the performance of the accumulation experiments. The global PHA productivity ($g_{PHA}/(L.d)$) was assessed by multiplying the fraction between the XPR and the SBR cycle length by the maximum PHA concentration achieved during the accumulation assays, divided by the time elapsed.

2.6. Biomass microbiome analysis

Biomass samples were collected from the SBR over each operating phase. The biomass was aseptically crushed and the resulting suspension was then used for genomic DNA extraction (DNeasy Power Soil kit, Qiagen). The 16S rRNA gene Microbiome Profiling with MiSeq was performed by Eurofins Genomics (Germany) by amplifying the hypervariable V3–V4 region using the primers set: 357F-TACGGGAGGCAGCAG and 800R-CCAGGGTATCTAATCC. The microbiome analysis was carried out according to Paulo et al. (2021).

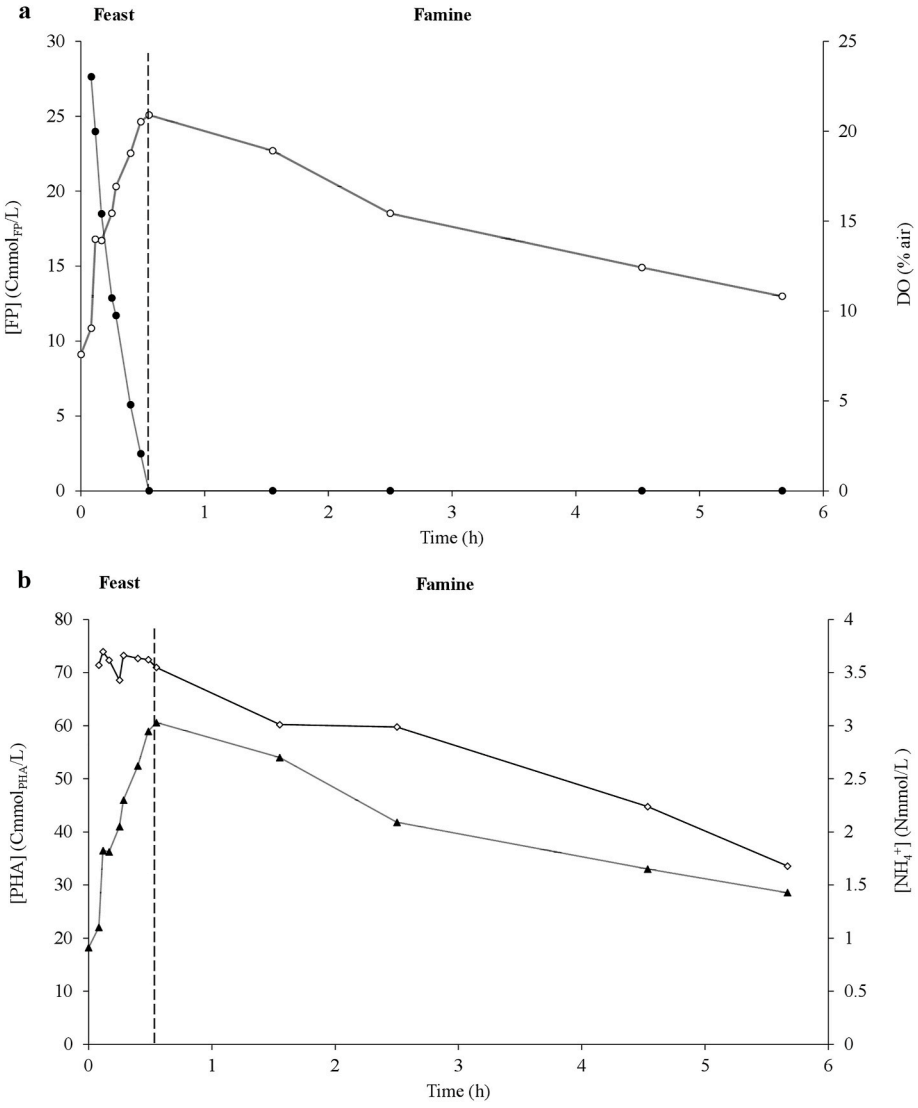

Fig. 1. Typical profile of an SBR cycle of biomass enriched during phase II. The variation of the FP concentrations (●) and the DO values (○) (a) and NH_4^+ (◇) and PHA (▲) contents (b) are presented. The dashed vertical line splits the feast and famine periods of the cycle.

3. Results and discussion

3.1. SBR performance over the culture selection phases

The SBR was operated during 6 months under different operating conditions, by subjecting the culture to cycles of feast (F) and famine (f) periods, aiming at enriching the biomass in PHA-storing organisms. The operating conditions were changed to improve the process productivity, namely to reach the highest PHA and biomass volumetric productivities. Throughout the selection of a PHA-storing culture, four different phases were established (phases I, II, III and IV), varying some operating parameters. On phase I, an OLR of 43.0 ± 1.5 $Cmmol_{FP}$/(L.d) was applied, which was further increased to 60.8 ± 6.0 $Cmmol_{FP}$/(L.d) on phase II, while keeping the other parameters. From phase II to III the SRT was decreased from 3.8 ± 0.1 to 2.0 ± 0.01 days, respectively, by maintaining the OLR at 64.8 ± 5.3 $Cmmol_{FP}$/(L.d). After *ca.* 5-months of operation, the SBR operation was stopped and the biomass was subjected to a starvation period of 3 months, mimicking a real case scenario of a plant shut down. Afterwards, the reactor operation was re-started on phase IV under the same conditions of phase II, as the highest global PHA productivity was attained on this phase, to ascertain on the capacity of the biomass to re-establish its biological activity after storage.

A typical SBR cycle started by feeding the culture with the FP, which are consumed along with oxygen during the feast period leading to the concomitant PHA accumulation (Fig. 1). Simultaneously to carbon exhaustion, a sudden increase of the DO level was observed, indicating the transition from the feast (maximum PHA content was achieved) to the famine period (Fig. 1a). During the famine period the intracellular polymer stored during the previous feast period was consumed along with NH_4^+ for cell growth and maintenance of the cellular viability (Fig. 1b).

The culture performance was assessed through the kinetic and stoichiometric parameters, calculated using data captured from at least 2 SBR monitoring cycles of each phase (Table 1). Through the Feast to famine (F/f) ratio it is possible to assess the selective pressure towards the selection of PHA-storing organisms. At the reactor start-up, during the first 25 days of operation, the F/f ratio decreased from 0.75 to 0.12 h/h (data not shown), corresponding to the acclimatization period of the culture. From this point onwards, the F/f ratio was quite stable (varying from 0.05 ± 0.01 to 0.08 ± 0.02 h/h) and below 0.2 h/h, the threshold value reported in the literature that assures the right selection pressure for the PHA-storing organisms (Duque et al., 2014). These results shows that neither the OLR nor SRT changes impacted the culture selection, which remained efficient towards the enrichment of PHA-storing organisms, corroborating the observations of previous works (Table 1) (Duque et al., 2014).

The SBR operation was first carried out under a low OLR of 43.0 ± 1.5 $Cmmol_{FP}$/(L.d) (Phase I) in order to acclimatize the culture to the feedstock and to avoid substrate inhibition. A specific FP consumption rate of 0.42 ± 0.10 $Cmmol_{FP}$/($Cmmol_{XA}$.h) was achieved, which was similar to the ones obtained using similar fermented streams and OLR (0.43 ± 0.05 $Cmmol_{FP}$/($Cmmol_{XA}$.h); 0.38 ± 0.06 $Cmmol_{FP}$/($Cmmol_{XA}$.h)) (Carvalheira et al., 2022; Duque et al., 2014). During the same period a specific PHA storage rate of 0.32 ± 0.09 $Cmmol_{PHA}$/($Cmmol_{XA}$.h) was achieved, which is within the range of the ones obtained using similar operating conditions (0.34 ± 0.04 $Cmmol_{PHA}$/($Cmmol_{XA}$.h)) or even higher (0.27 ± 0.05 $Cmmol_{PHA}$/($Cmmol_{XA}$.h)) (Carvalheira et al., 2022; Duque et al., 2014), resulting in a PHA yield of 0.78 ± 0.05 $Cmmol_{PHA}$/$Cmmol_{FP}$. Furthermore, a biomass volumetric productivity (XPR) of 0.57 ± 0.20 g_{XA}/(L.d)) was achieved during phase I (Table 1).

Aiming at increasing the PHA process productivity, the OLR was increased to 60.8 ± 6.0 $Cmmol_{FP}$/(L.d) on phase II. Higher OLRs usually lead to higher biomass concentrations, which in turn enables the selection of higher numbers of PHA-storers microorganisms and thus, improves PHA process productivity (Albuquerque et al., 2010; Carvalheira et al., 2022). As observed in other studies, the kinetic parameters were independent of the range of OLR tested as no relevant differences were observed on both FP consumption and PHA production specific rates with the OLR increase (Carvalheira et al., 2022). On the other hand, the PHA volumetric productivity (r_{PHA}) more than doubled and a PHA yield of 0.83 ± 0.07 $Cmmol_{PHA}$/$Cmmol_{FP}$ was achieved (Table 1). Using similar operating conditions but different feedstocks, lower PHA yields of *ca.* 0.66 ± 0.15 and 0.78 ± 0.22 $Cmmol_{PHA}$/$Cmmol_{FP}$ for fermented sugar cane molasses and fermented cheese whey, respectively, were obtained (Duque et al., 2014). Furthermore, the OLR increase seemed to greatly impact the XPR, which increased almost 2 times from 0.57 ± 0.20 on phase I to 1.09 ± 0.11 g_{XA}/(L.d) on phase II (Table 1). This led to an increase of the X_A concentration due to the availability of more external carbon source (Table 1). These findings were also reported by some authors, where higher biomass productivities were achieved at higher OLR due to the high biomass concentrations within the systems (Carvalheira et al., 2022; Matos et al., 2021b). The higher XPR means that more biomass is available to produce PHA, which can in turn increase the PHA productivity, leading to a higher amount of PHA produced (Cruz et al., 2022). The results corroborate this statement as a higher PHA concentration was observed on phase II comparing to phase I (0.70 ± 0.2 and 1.12 ± 0.2 g_{PHA}/L, on phase I and II, respectively) (Table 1).

The decrease of the SRT from 3.8 ± 0.1 days on phase II to 2.0 ± 0.01 days on phase III seemed to achieve the highest specific FP consumption (0.53 ± 0.09 $Cmmol_{FP}$/($Cmmol_{XA}$.h)) and PHA storage (0.45 ± 0.06 $Cmmol_{PHA}$/($Cmmol_{XA}$.h)) rates. However, considering the standard deviation, the average values were within the same range of those obtained for phases I and II (Table 1). Instead, the volumetric PHA productivity and the X_A concentration decreased (Table 1). This finding is in agreement with that reported by Matos et al. (2021b), where using the same OLR, lower X_A concentrations were observed under the lower SRT (2 days versus 4 days). In fact, lowering the SRT increases the XPR but lead to a decrease in the X_A concentration (Table 1). However, as the same OLR of phase II was applied on phase III, the PHA content increased from 18.4 ± 2.1% g_{PHA}/g_{TS} on phase II to its maximum of 24.5 ± 3.8% g_{PHA}/g_{TS} on phase III due to the lower X_A concentration, but the PHA concentration remained similar (1.12 ± 0.2 and 1.02 ± 0.2 g_{PHA}/L on phase II and III, respectively) (Table 1).

On phase IV the SBR was re-inoculated with the biomass stored for 3 months. Shortly after reinoculation, the biomass biological activity was re-activated. After the starvation period, on phase IV the SBR was reactivated and operated under the same conditions applied of phase II (Table 1). Once the steady state was achieved, the SBR cycles were monitored and the results showed that the starvation period seemed to impact the FP consumption and PHA production specific rates as the lowest values of 0.33 ± 0.01 $Cmmol_{FP}$/($Cmmol_{XA}$.h) and 0.27 ± 0.01 $Cmmol_{PHA}$/($Cmmol_{XA}$.h) were achieved, respectively (Table 1). However, they are still in the range of the ones already reported by other authors using similar conditions (Carvalheira et al., 2022; Duque et al., 2014). Despite that, the same PHA yield of phase II and III was achieved (0.83 ± 0.004 $Cmmol_{PHA}$/$Cmmol_{FP}$) and over time a re-establishment of the X_A concentration was observed, which became similar to the one attained on phase II (4.4 ± 0.7 and 4.1 ± 0.5 g_{XA}/(L.d) on phases IV and II, respectively) (Table 1). Furthermore, the PHA concentration was also similar to the one achieved on phases II and III (1.03 ± 0.2 g_{PHA}/L on average for phases II, III and IV), meaning that although the culture selected on the previous phases showed a slower performance on phase IV, it was able to recover its biological activity in terms of PHA yield and concentration to values similar to the ones obtained in phase II, demonstrating the robustness of the culture and its reactivation capacity after storage (Table 1). Moreover, the ability of the culture to regain its PHA producing activity proves that the culture storage can be a good way to preserve the biomass in case of system shut down, avoiding the need to perform a new culture selection process to restart the process, which is highly time consuming.

Throughout the SBR operation, NH_4^+ was available during the entire

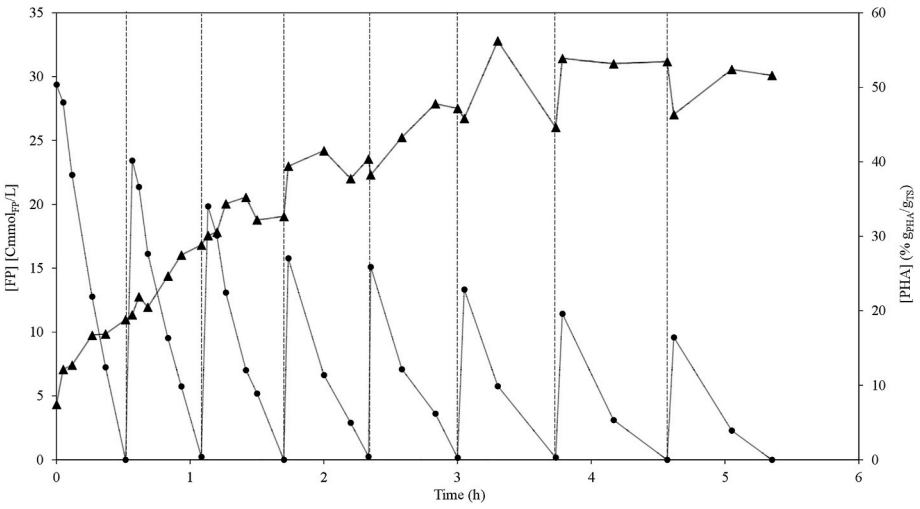

Fig. 2. Typical profile of an accumulation assay performed with the operating conditions of phase II. Eight pulse feedings were performed and each pulse feeding cycle is delimited by the dashed vertical lines. The FP concentration (Cmmol$_{FP}$/L) (●) and the PHA content (% g$_{PHA}$/g$_{TS}$) (▲) are presented.

cycle (feast and famine periods), meaning that in the absence of a selective pressure towards the PHA-storing organisms, the carbon could be consumed together with NH_4^+ by the non-storing organisms to grow during the feast period, instead of being used by the PHA-storing organisms to accumulate PHA. Contrarily, if a proper selective pressure is applied, the PHA-storing organisms can faster uptake the substrate rather than the non PHA-storing organisms (Albuquerque et al., 2010). In this work, no relevant NH_4^+ consumption neither biomass growth were observed during the feast period comparing to the famine period. Indeed, NH_4^+ started to be relevantly consumed immediately after the carbon depletion (beginning of the famine period), but it was not totally consumed (Fig. 1b). The NH_4^+ and the intracellular PHA were simultaneously consumed as sources of carbon, energy and nutrients needed for cell growth and proliferation (Albuquerque et al., 2007). A similar trend was observed by Johnson et al. (2010) using a similar C:N ratio of 11 Cmol:Nmol, with the culture showing a carbon-limited behaviour instead of a nitrogen-limited one.

Throughout the SBR operation and independently of the phase, a similar pattern for the consumption of the different FP in the mixture was observed. The culture preferentially consumed the HBut (overall average of 0.21 ± 0.06 Cmmol$_{HBut}$/(Cmmol$_{XA}$.h)), followed by the HAc (overall average of 0.13 ± 0.03 Cmmol$_{HAc}$/(Cmmol$_{XA}$.h) and HCap (overall average of 0.09 ± 0.02 Cmmol$_{HCap}$/(Cmmol$_{XA}$.h)) (data not shown). In fact, one of the compounds faster consumed is the HBut, whose consumption is often considered more energetically efficient than the consumption of the other FP also present in the mixture (Carvalheira et al., 2022; Marang et al., 2013; Matos et al., 2021b).

Regardless of the phase and thus, of the operating conditions, the major polymer components were the 3HB monomers (75–79% Cmol), followed by the 3HV (10–13% Cmol), the 3HHx (5–9% Cmol) and the

Table 2
Kinetic and stoichiometric parameters achieved during the PHA accumulation assays conducted with biomass enriched in each SBR phase. Values are means ± standard deviations.

	Phase I	Phase II	Phase III		Phase IV
Pulses concentration (Cmmol$_{FP}$/L)	16.6 ± 1.3	22.8 ± 2.3	17.7 ± 2.5		23.5 ± 5.1
-q$_{FPmax}$[a] (Cmmol$_{FP}$/(Cmmol$_{XA}$.h))	0.38 ± 0.08	0.49 ± 0.07	0.64 ± 0.10		0.42 ± 0.02
q$_{PHAmax}$[a] (Cmmol$_{PHA}$/(Cmmol$_{XA}$.h))	0.31 ± 0.07	0.35 ± 0.03	0.45 ± 0.13		0.36 ± 0.04
Y$_{PHA/FPmax}$[a] Cmmol$_{PHA}$/Cmmol$_{FP}$)	0.79 ± 0.02	0.71 ± 0.04	0.72 ± 0.13	**Starvation period**	0.81 ± 0.08
PHA$_{max}$ (% g$_{PHA}$/g$_{TS}$)	45.7 ± 6.6	45.4 ± 7.1	44.8 ± 5.2		43.9 ± 0.5
Global PHA productivity (g$_{PHA}$/(L.d))	1.23 ± 0.3	3.55 ± 0.8	2.57 ± 0.1		3.01 ± 0.4
Polymer composition (% Cmol)					
3HB	85 ± 1	82 ± 1	77 ± 5		82 ± 1
3HV	10 ± 2	12 ± 1	13 ± 2		14 ± 1
3H2MV	1 ± 0.1	1 ± 0.3	1 ± 0.2		1 ± 0.002
3HHx	5 ± 1	5 ± 1	8 ± 2		3 ± 0.5

[a] calculated for the two first pulses

3H2MV (3–5% Cmol) monomers (Table 1). Thus, a quarter-polymer composed by 4 different monomers was obtained, which is of great interest as they can enhance the flexibility and the resistance of the final polymer (Loo and Sudesh, 2007; Silva et al., 2022; Zhila and Shishatskaya, 2018). As the FP are PHA precursors, the composition of the fBSG used as feedstock directly affects the final polymer composition. In fact, if the fBSG composition did not vary over time, no relevant changes on the polymer composition were expected. However, the different operating conditions applied along the SBR operation could also contribute for the polymer composition. Nevertheless, no major changes were observed on the polymer composition along the different phases, meaning that the amount of each monomer and thus, the polymer composition, are independent of the applied OLR and SRT. Furthermore, even after the reactivation process the polymer had a similar composition to the ones observed in previous phases.

3.2. PHA accumulation assays

The PHA accumulation assays were performed with biomass collected at the pseudo-steady state of each SBR phase. Typical FP and PHA content profiles along an accumulation assay using a pulse feeding strategy, where the FP consumption and concomitant PHA production occur, is presented in Fig. 2.

The different operating conditions can lead to different culture performances and thus, on each operating phase, the maximum capacity of the biomass to accumulate PHA was assessed during the accumulation assays (Table 2). The performance of the enriched culture on phases I and II during the PHA accumulation assays was like the one achieved during the culture selection (similar maximum specific FP and PHA rates (Tables 1 and 2). The highest maximum specific FP consumption (0.64 ± 0.10 $Cmmol_{FP}/(Cmmol_{XA}.h)$ and PHA storage (0.45 ± 0.13 $Cmmol_{PHA}/(Cmmol_{XA}.h)$ rates were achieved using biomass enriched on phase III, which is also in accordance with the results obtained in the culture selection (Tables 1 and 2). On phase IV, after the starvation period, the specific rates were slightly higher than the ones observed over SBR operation but were similar to the ones achieved on phase II (operated under the same conditions).

Concerning the PHA yields, in opposite to the observed on phases I and IV which had similar values of PHA yields in both selection and accumulation stages, lower PHA yields were observed on the accumulation assays from phases II and III than in the selection stage. Due to the lack of online tools to directly monitor the PHA content, the addition of new pulses of carbon during the PHA accumulation assays was monitored through the DO values (indirect PHA monitoring), which can lead to a lately addition of a new pulse and consequently, to some PHA consumption during the pulses (Table 2). Nevertheless, the values obtained in the present work are within the range of PHA yields or even higher than the ones described in the literature by several authors (up to 0.70 $Cmmol_{PHA}/Cmmol_{FP}$) using similar operating conditions (Carvalheira et al., 2022; Duque et al., 2014). The maximum PHA content was very similar in each phase, varying from 43.9 ± 0.5 to 45.7 ± 6.6% g_{PHA}/g_{TS} (on average) (Table 2). Regardless of the phase, the polymer remained mainly composed by 3HB monomers (81.5% Cmol on average). The 3HV, 3HHx and 3H2MV monomers were also present in the polymer composition, albeit at lower percentages (12.3, 5.3 and 1% Cmol, on average, respectively). Comparing with the polymer composition produced during the SBR operation, the 3HB content seemed to slightly increase, whereas the content of 3H2MV decreased.

The global PHA productivity, evaluated taking into account the selection and the accumulations stages, ranged from 1.23 to 3.55 $g_{PHA}/(L.d)$, which are within the range of PHA productivities reported in previous studies (0.73–8.1 $g_{PHA}/(L.d)$) (Cruz et al., 2022; Matos et al.,

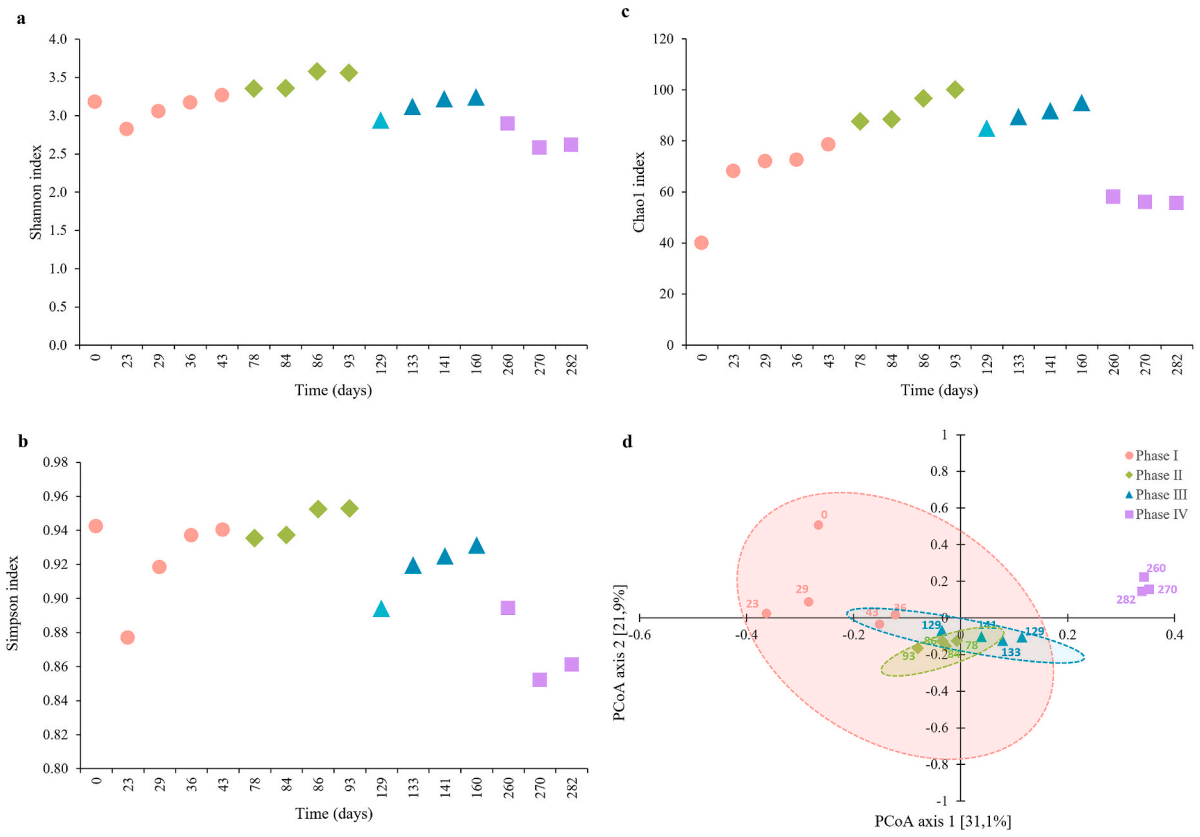

Fig. 3. Alpha diversity of the biomass bacterial community over time represented by (a) Shannon index; (b) Simpson index and (c) Chao1 index. (d) PCoA plot of beta-diversity based on Bray-Curtis distance (PERMANOVA; $F = 6.09$, $R^2 = 0.58$, $p < 0.001$). The samples of each phase are represented as follows: ● Phase I; ◆ Phase II; ▲ Phase III and ■ Phase IV.

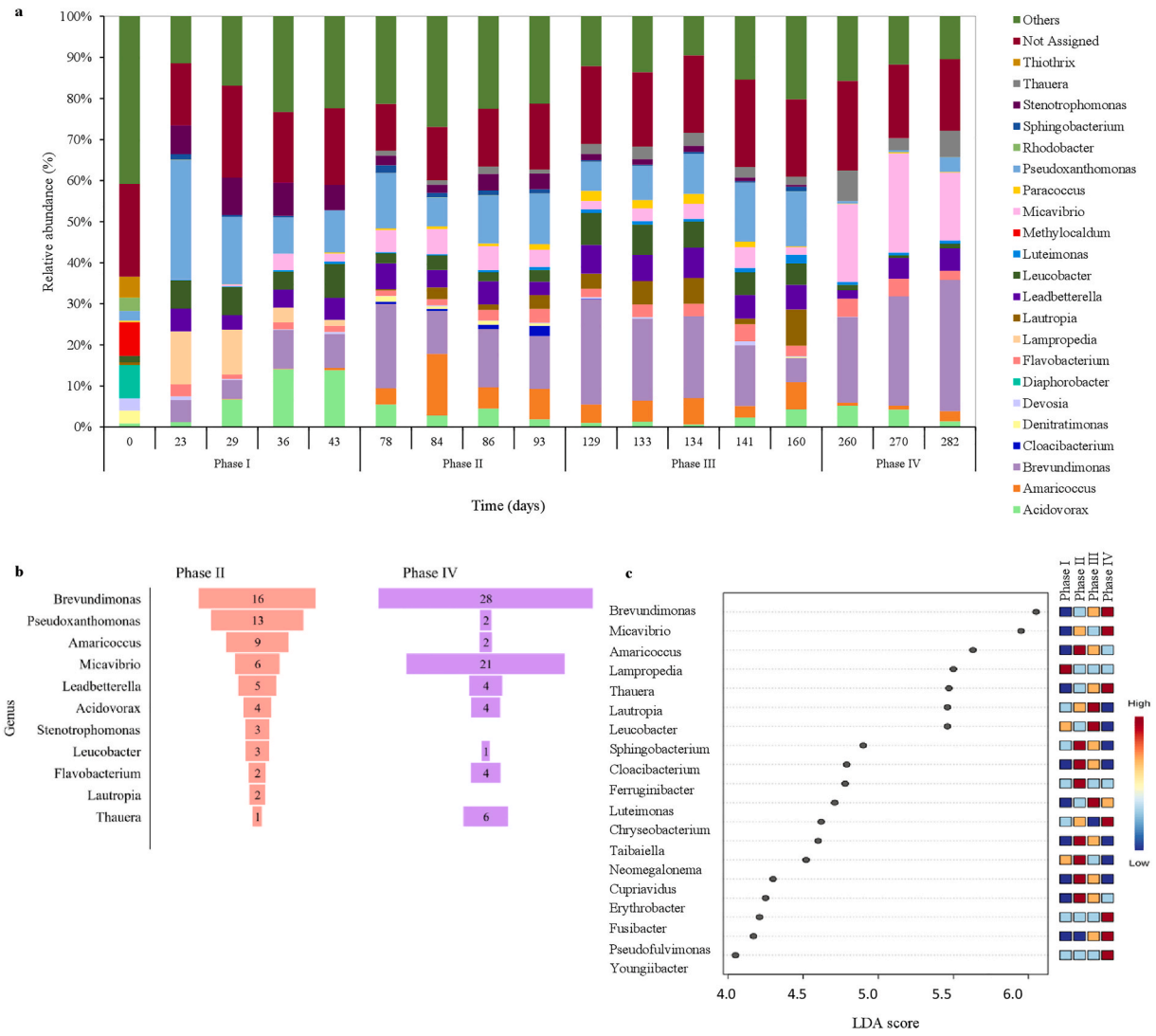

Fig. 4. Taxonomic composition of the bacterial community over reactor operation. (a) The relative abundance of bacterial communities at the genus level on different sampling days presenting the genera with relative abundance ≥2% on at least one day. The remaining genera present in biomass but with a relative abundance <2% on all sampling days are included in the group "Others" whereas taxa not assigned to a specific genus are included in the group "Not assigned". (b) The top 10 most abundant genus of phases II and IV and their averaged relative abundance in those phases. (c) LEfSe of the bacteriome present in the SBR biomass at genus level (LDA score >4.0; p-value<0.05). The significant genera were ranked in declining order as per their LDA scores (x-axis).

2021a, 2021b; Oliveira et al., 2017). The OLR increase, within the range studied in the present work, positively benefits the overall process as higher rates, biomass and PHA productivities were achieved (Tables 1 and 2). The highest global PHA productivity (3.55 ± 0.8 g_{PHA}/(L.d)) was attained on phase II with a culture selected under a SRT of 4 days. The subsequent decrease of the SRT to 2 days led to a decrease of the global PHA productivity to 2.57 ± 0.1 g_{PHA}/(L.d), due to the decrease on the amount of X_A on phase III (Table 2). A similar trend was reported by other authors (Matos et al., 2021b). Furthermore, after the starvation period, although a slightly lower global PHA productivity (3.01 ± 0.4 g_{PHA}/(L.d)) was achieved, which was similar within the error to the one achieved in phase II (3.55 ± 0.8 g_{PHA}/(L.d)) (Table 2), the selected culture was able to reactivate its PHA synthetizing capacity, demonstrating its robustness.

3.3. Microbiome dynamics over the culture selection phases in the SBR

3.3.1. Alpha- and beta-diversity over time

To evaluate the changes of the SBR biomass microbiome over operation, the alpha- and beta-diversity metrics of the bacterial community were investigated (Fig. 3). Alpha diversity, based on the Shannon index that measures the diversity of species within a community, indicated that the inoculum bacterial community was highly diverse (Fig. 3a). Although an initial perturbation can be observed, the species diversity in the biomass community increased progressively over phases I and II. On phase III and IV slightly lower Shannon indices were observed in comparison to phase II, indicating that the bacterial community on those days was less diverse, which in part could be due to the biomass specialization over time (Fig. 3a). The Simpson index is a diversity estimator that considers species evenness more than species richness in its measurement thus reflecting on species dominance. The variation of the Simpson indices over time followed a similar pattern of the Shannon indices, where samples by the end of phase II had the highest indices values whereas the ones of phase IV had the lowest ones (Fig. 3b). This reveals that although the biomass during phase IV was still able to effectively produce PHA (according to Table 1), on phase II a higher PHA volumetric productivity was achieved, which coincided with a more even microbiome population (Table 1). The storage process could have contributed for the selection of a less even microbiome population that was still able to produce PHA, albeit at a lower rate as previously

observed in the performance results (Table 1). To estimate species richness, the Chao index which indicates the predicted total number of microbial species within the biomass was used (Fig. 3c). The inoculum presented a lower bacterial richness but along phases I and II, the biomass richness progressively increased. On the other hand, the Chao indices observed for samples of phase IV were lower in comparison with the ones from samples of previous phases (Fig. 3c). This decrease on the biomass richness was probably because of the storage period, as perhaps some taxa were not able to recover its abundance in the biomass during the reactor reactivation.

The beta-diversity of the bacterial community provides a measure of the distance or dissimilarity between biomass samples. The Principal Coordinates Analysis (PCoA) based on Bray-Curtis dissimilarity matrix, performed at genus level, showed that the composition of bacterial communities varied over time, with samples being mostly separated along the x-axis (Fig. 3d). In general, the closer the samples are plotted, the more similar their community compositions are. The biomass composition at the early beginning of operation (till day 29) was clearly different from that on the subsequent days of phase I, which were much close to each other. This result reveals the acclimation process that the inoculum suffered over the first month of reactor operation. For biomass collected throughout phases II and III, samples from the same phase clustered together. However, the samples from phase II had a shorter Bray-Curtis distance from themselves than the samples from phase III. The closer distance between the biomass samples from those phases indicates that the variations in the community structure were relatively small, whereas the close location of samples within the same phase reveals that the biomass of each phase has a somewhat distinct bacterial population signature. Samples from phase IV also clustered together, but separately from the remaining samples, indicating that the biomass microbiome established after the reactor reactivation was slightly different from the one present before the storage period.

3.3.2. Microbiota composition changes over the culture selection phases

The biomass microbiome composition at genus level over the SBR operation shows that shifts in the biomass microbiome composition were evident, especially in phase I (Fig. 4a). The bacterial community within the inoculum was remarkably different from that on the subsequent days of that phase, although it became more similar by the end of phase I (days 36 and 43). This is in accordance with the PCoA that indicated a clear separation between the inoculum and the biomass samples at the end of phase I. Taxa belonging to *Denitratimonas*, *Devosia*, *Diaphorobacter*, *Methylocaldum*, *Rhodobacter* and *Thiothrix* genera were present in the inoculum, but over operation their relative abundance tended to decrease or to be completely vanished from the biomass. On the contrary, taxa from the genera *Acidovorax*, *Lautropia*, *Leucobacter*, *Paracoccus* and *Pseudoxanthomonas* were present in the inoculum at low relative abundancies but over operation their relative abundance tended to increase. This increase was especially relevant for the *Pseudoxanthomonas* genus, which became one of the most abundant taxa in the microbiome (except in phase IV) (Fig. 4a).

The analysis of the biomass taxonomic composition over operation showed a different profile in terms of microbial composition under the different tested conditions, indicating that in each phase a distinct assemblage of taxa existed. Overall, after an acclimation period, the system was able to enrich the biomass in distinct well known PHA-storing microorganisms, such as *Acidovorax* (Pereira et al., 2020), *Amaricoccus* (Rangel et al., 2023), *Brevundimonas* (Liang et al., 2023), *Stenotrophomonas* (Cruz et al., 2022), *Leucobacter* (Clagnan and Adani, 2023), *Leadbetterella* (Clagnan and Adani, 2023) and *Thauera* (Yin et al., 2018) genera. The biomass microbiome in each phase comprised most of those genera known to have metabolic ability for synthesizing PHA, but their relative abundance oscillated depending on the operating conditions applied. In fact, by the end of phase I, *Acidovorax* was the most common genus (16%, in average), followed by *Pseudoxanthomonas* (11%), *Brevundimonas* (10%), *Stenotrophomonas* (8%), *Leucobacter* (7%) and *Leadbetterella* (6%) (Fig. 4a). Although the *Pseudoxanthomonas* genus was the genus second most abundant in the microbiome on that day, this genus PHA storing ability is not well documented in the literature yet. Ghribi et al. (2016) isolated from paper mill sludge a bacterial strain of the *Pseudoxanthomonas* genus that exhibited PHA production potential based on staining with Sudan black B and Nile blue A tests. Remarkably, this genus has been found in high proportion in microbiomes of MMC systems, thus suggesting that its role is somehow linked to PHA production (Clagnan and Adani, 2023; Portela-Grandío et al., 2021).

After increasing the OLR in phase II, changes in the abundance of the main genera were observed. The genus *Acidovorax* lost its predominance in the biomass composition, achieving a relative abundance of 2% by the end of that phase and giving place to the genera *Pseudoxanthomonas* and *Brevundimonas* which became the most abundant taxa, each representing about 14% of the relative abundance of the total abundance. The *Micavibrio* genus slightly increased in abundance whereas *Leadbetterella*, *Leucobacter* and *Stenotrophomonas* decreased (Fig. 4a). The *Acidovorax* genus is a well-known PHA producer that was found in high abundance in a mixed microbial culture system dedicated to the production of PHA using fermented waste streams from a pulp and paper factory as feedstock (Pereira et al., 2020). Interestingly, similarly to that we observed in the present study, the relative abundance of this genus also decreased with the increase of the OLR. Furthermore, the genus *Amaricoccus*, which was underrepresented in phase I (less than 1%), augmented its relative abundance to about 8% by the end of phase II. In a study conducted by Rangel et al. (2023), a similar trend in which this genus relative abundance increased in consequence of the OLR increase was observed, suggesting that this organism proliferation within the overall microbiome is favoured by higher organic loads.

After shortening the SRT to 2 days in phase III, the *Pseudoxanthomonas* genus maintained its relative abundance on the overall community, whereas the one of the *Brevundimonas* genus initially increased but by the end of that phase it was reduced to about half in comparison to phase II. On the contrary, several other bacterial genus taxa increased their relative abundances (e.g., *Lautropia*, *Leadbetterella*, *Leucobacter*, *Luteimonas* and *Thauera*) (Fig. 4a). On phase IV, although the OLR and SRT applied were like those on phase II, the biomass microbiome by the end of this phase was dominated by two bacteria genera: *Brevundimonas* (33%) and *Micavibrio* (17%) (Fig. 4a). Although the high proportion of members of the *Micavibrio* genus on phase IV, to the best of our knowledge there are no reports on their PHA production ability. Indeed, this genus has been reported as an obligate epibiotic predator for many Gram-negative bacteria, capable to attach to the outer membrane of their prey, completely or partly consuming prey cells (Pasternak et al., 2014). Taxa closely related to the *Micavibrio*-like bacterium were identified in biomass from reactors and in freshwater, soil, and extreme environments (Dolinšek et al., 2013). Nevertheless, the biomass still has in its bacterial composition several known PHA-accumulators such as the *Brevundimonas* genus in high abundance, and members affiliated with the *Acidovorax*, *Amaricoccus*, *Leadbetterella* and *Thauera* genera were also found in the microbiome, albeit at lower relative abundance (up to 7%). The high abundance of the *Micavibrio* genus over phase IV could have contributed for the slightly lower PHA volumetric productivity during culture selection, thus corroborating the performance results. A more detailed analysis of the genus taxa profile on both phases, based on their relative abundance, revealed the prevalence of a distinct taxonomic composition pattern (Fig. 4b). After reactor reactivation (phase IV), a more specialized community was developed with *Brevundimonas* and *Micavibrio* genera dominant in terms of relative abundance, which is in line with the alpha diversity indices, that showed that the community diversity and richness decreased. This shift on the biomass composition could be explained by the storage process, as perhaps during the biomass reactivation some taxa, including some PHA-accumulators, were not able to thrive in the community, triggering changes in diversity.

Additionally, a linear discriminant analysis effect size (LEfSE) was performed to investigate the statistically significant differences in the biomass bacterial community (at genus level) among the operating phases. The LEfSE allowed to identify the bacterial fingerprint of each phase (i.e., the phase-specific taxa by comparing the taxa abundances between different phases) (Fig. 4c). For instance, the genus *Amaricoccus* was significantly abundant in phase II (LDA of 5.63, $p = 0.004$) in comparison to other phases and thus, was the most prominent biomarker of this phase. Nevertheless, there are other taxa which also characterize this phase, namely the *Sphingobacterium*, *Cloacibacterium*, *Ferruginibacter*, *Taibaiella*, *Neomegalonema*, *Cupriavidus* and *Erythrobacter*, although at lower LDA score. On phase III, the genera *Lautropia*, *Leucobacter* and *Luteimonas* were the most prevalent features that differentiate this phase from the others (Fig. 4c). Concerning phase IV, among the 7 representative genera pinpointed as potential biomarkers for this phase, the *Brevundimonas*, *Micavibrio* and *Thauera* genera were the ones that best characterize this phase (Fig. 4c). Although LEfSE highlighted the specific bacterial taxa that most characterize each phase, most of those genera were shared between the different phases, but their abundance differed. The identification of the specific taxa which were significantly enriched in each phase, helps to understand the adaptive response of the bacterial community to the different operating conditions.

In general, the microbiome of the biomass of the culture selection reactor harbours multiple genera of PHA producers and, in each phase most of those genera persisted in the microbiome, but their relative abundance oscillated depending on the operating conditions applied. In fact, the changes of the operating conditions shifted the proportion of the various PHA-producers in the biomass, thus creating a specific signature for each phase, which in turn affected the global PHA productivity.

4. Conclusions

An efficient PHA-accumulating MMC was enriched using fermented brewer's spent grain as feedstock. The maximum global PHA productivity (3.55 ± 0.8 g_{PHA}/(L.d)) was achieved at an OLR of 60.8 ± 6.0 $Cmmol_{FP}$/(L.d) and a SRT of 3.8 ± 0.1 days. After storage, the biomass restored its PHA-synthetizing activity, achieving a similar productivity to that obtained before in similar conditions. The microbiome structure and composition changed according to the operating conditions. Although most genera related to PHA production persisted in the microbiome, their relative abundance varied. Each phase has its own biomarkers and thus, a distinct bacterial population signature.

CRediT authorship contribution statement

Eliana C. Guarda: Conceptualization, Data curation, Formal analysis, Investigation, Writing – original draft. **Catarina L. Amorim:** Data curation, Formal analysis, Writing – original draft. **Gabriele Pasculli:** Data curation, Formal analysis. **Paula M.L. Castro:** Funding acquisition, Writing – review & editing. **Claudia F. Galinha:** Conceptualization, Funding acquisition, Supervision, Writing – review & editing. **Anouk F. Duque:** Conceptualization, Funding acquisition, Supervision, Writing – review & editing. **Maria A.M. Reis:** Conceptualization, Funding acquisition, Supervision, Writing – review & editing.

Declaration of competing interest

The authors declare that they have no known competing financial interests or personal relationships that could have appeared to influence the work reported in this paper.

Data availability

Data will be made available on request.

Acknowledgments

This work was financed by national funds from FCT - Fundação para a Ciência e a Tecnologia, I.P., in the scope of the projects Beer2BioPol-PTDC/BTA-BTA/31746/2017, UIDP/04378/2020 and UIDB/04378/2020 of UCIBIO, LA/P/0140/2020 of i4HB, and UIDB/50016/2020 of CBQF. This work was also supported by LAQV, which is financed by national funds from FCT/MCTES (LA/P/0008/2020, UIDP/50006/2020 and UIDB/50006/2020). The authors gratefully acknowledge FCT for the financial support through the PhD grants SFRH/BD/136300/2018 + COVID/BD/153202/2023 (E.C. Guarda), Scientific Employment Stimulus - Individual Call (2022.04601.CEECIND –C.F. Galinha) and program DL 57/2016 – Norma transitória (C.L. Amorim and A.F. Duque).

References

Albuquerque, M.G.E., Eiroa, M., Torres, C., Nunes, B.R., Reis, M.A.M., 2007. Strategies for the development of a side stream process for polyhydroxyalkanoate (PHA) production from sugar cane molasses. J. Biotechnol. 130, 411–421. https://doi.org/10.1016/j.jbiotec.2007.05.011.

Albuquerque, M.G.E., Torres, C.A.V., Reis, M.A.M., 2010. Polyhydroxyalkanoate (PHA) production by a mixed microbial culture using sugar molasses: effect of the influent substrate concentration on culture selection. Water Res. 44, 3419–3433. https://doi.org/10.1016/j.watres.2010.03.021.

Apha, S.M., 2012. Standard methods for the examination of water and wastewater. Publ. Health 51, 940, 940.

Carvalheira, M., Amorim, C.L., Oliveira, A.C., Guarda, E.C., Costa, E., Ribau Teixeira, M., Castro, P.M.L., Duque, A.F., Reis, M.A.M., 2022. Valorization of brewery waste through polyhydroxyalkanoates production supported by a metabolic specialized microbiome. Life 12, 1–14. https://doi.org/10.3390/life12091347.

Clagnan, E., Adani, F., 2023. Influence of feedstock source on the development of polyhydroxyalkanoates-producing mixed microbial cultures in continuously stirred tank reactors. N. Biotech. 76, 90–97. https://doi.org/10.1016/j.nbt.2023.05.005.

Crutchik, D., Franchi, O., Caminos, L., Jeison, D., Belmonte, M., Pedrouso, A., Val del Rio, A., Mosquera-Corral, A., Campos, J.L., 2020. Polyhydroxyalkanoates (PHAs) production: a feasible economic option for the treatment of sewage sludge in municipalwastewater treatment plants? Water (Switzerland) 12, 1–12. https://doi.org/10.3390/W12041118.

Cruz, R.A.P., Oehmen, A., Reis, M.A.M., 2022. The impact of biomass withdrawal strategy on the biomass selection and polyhydroxyalkanoates accumulation of mixed microbial cultures. New Biotechnolo. The impact of biomass withdrawal strategy on the bioCruzR. A. P., Oehmen, A., & Reis, M. A. M. (2022). N. Biotech. 66, 8–15. https://doi.org/10.1016/j.nbt.2021.08.004.

Dolinšek, J., Lagkouvardos, I., Wanek, W., Wagner, M., Daims, H., 2013. Interactions of nitrifying bacteria and heterotrophs: identification of a Micavibrio-like putative predator of Nitrospira spp. Appl. Environ. Microbiol. 79, 2027–2037. https://doi.org/10.1128/AEM.03408-12.

Duque, A.F., Oliveira, C.S.S., Carmo, I.T.D., Gouveia, A.R., Pardelha, F., Ramos, A.M., Reis, M.A.M., 2014. Response of a three-stage process for PHA production by mixed microbial cultures to feedstock shift: impact on polymer composition. N. Biotech. 31, 276–288. https://doi.org/10.1016/j.nbt.2013.10.010.

European Bioplastics, 2022. Bioplastic Market Development Update 2022.

Ghribi, M., Meddeb-Mouelhi, F., Beauregard, M., 2016. Microbial diversity in various types of paper mill sludge: identification of enzyme activities with potential industrial applications. SpringerPlus 5. https://doi.org/10.1186/s40064-016-3147-8.

Guarda, E.C., Costa, E., Gil, C., Amorim, C.L., Galinha, C., Duque, A.F., Castro, P.M.L., Reis, M.A.M., 2023. Acidogenic fermentation of brewers' spent grain: performance and monitoring through two-dimensional fluorescence spectroscopy. ACS Sustain. Chem. Eng. https://doi.org/10.1021/acssuschemeng.3c00316.

Gurieff, N., Lant, P., 2007. Comparative life cycle assessment and financial analysis of mixed culture polyhydroxyalkanoate production. Bioresour. Technol. 98, 3393–3403. https://doi.org/10.1016/j.biortech.2006.10.046.

Johnson, K., Kleerebezem, R., van Loosdrecht, M.C.M., 2010. Influence of the C/N ratio on the performance of polyhydroxybutyrate (PHB) producing sequencing batch reactors at short SRTs. Water Res. 44, 2141–2152. https://doi.org/10.1016/j.watres.2009.12.031.

Liang, B., Zhang, X., Wang, F., Miao, C., Ji, Y., Huang, Z., Gu, P., Liu, X., Fan, X., Li, Q., 2023. Production of polyhydroxyalkanoate by mixed cultivation of Brevundimonas diminuta R79 and Pseudomonas balearica R90. Int. J. Biol. Macromol. 234, 123667 https://doi.org/10.1016/j.ijbiomac.2023.123667.

Loo, C., Sudesh, K., 2007. Polyhydroxyalkanoates : bio-based microbial plastics and their properties. Malaysian Polym. J. 2, 31–57.

Marang, L., Jiang, Y., van Loosdrecht, M.C.M., Kleerebezem, R., 2013. Butyrate as preferred substrate for polyhydroxybutyrate production. Bioresour. Technol. 142, 232–239. https://doi.org/10.1016/j.biortech.2013.05.031.

Matos, M., Cruz, R.A.P., Cardoso, P., Silva, F., Freitas, E.B., Carvalho, G., Reis, M.A.M., 2021a. Combined strategies to boost polyhydroxyalkanoate production from fruit waste in a three-stage pilot plant. ACS Sustain. Chem. Eng. 9, 8270–8279. https://doi.org/10.1021/acssuschemeng.1c02432.

Matos, M., Cruz, R.A.P., Cardoso, P., Silva, F., Freitas, E.B., Carvalho, G., Reis, M.A.M., 2021b. Sludge retention time impacts on polyhydroxyalkanoate productivity in uncoupled storage/growth processes. Sci. Total Environ. 799, 149363 https://doi.org/10.1016/j.scitotenv.2021.149363.

Oehmen, A., Keller-Lehmann, B., Zeng, R.J., Yuan, Z., Keller, J., 2005. Optimisation of poly-β-hydroxyalkanoate analysis using gas chromatography for enhanced biological phosphorus removal systems. J. Chromatogr. A 1070, 131–136. https://doi.org/10.1016/j.chroma.2005.02.020.

Oliveira, C.S.S., Silva, C.E., Carvalho, G., Reis, M.A., 2017. Strategies for efficiently selecting PHA producing mixed microbial cultures using complex feedstocks: feast and famine regime and uncoupled carbon and nitrogen availabilities. N. Biotech. 37, 69–79. https://doi.org/10.1016/j.nbt.2016.10.008.

Pasternak, Z., Njagi, M., Shani, Y., Chanyi, R., Rotem, O., Lurie-Weinberger, M.N., Koval, S., Pietrokovski, S., Gophna, U., Jurkevitch, E., 2014. In and out: an analysis of epibiotic vs periplasmic bacterial predators. ISME J. 8, 625–635. https://doi.org/10.1038/ismej.2013.164.

Paulo, A.M.S., Amorim, C.L., Costa, J., Mesquita, D.P., Ferreira, E.C., Castro, P.M.L., 2021. Long-term stability of a non-adapted aerobic granular sludge process treating fish canning wastewater associated to EPS producers in the core microbiome. Sci. Total Environ. 756, 144007 https://doi.org/10.1016/j.scitotenv.2020.144007.

Pereira, J., Queirós, D., Lemos, P.C., Rossetti, S., Serafim, L.S., 2020. Enrichment of a mixed microbial culture of PHA-storing microorganisms by using fermented hardwood spent sulfite liquor. N. Biotech. 56, 79–86. https://doi.org/10.1016/j.nbt.2019.12.003.

Pereira, J.R., Rafael, A.M., Esmail, A., Morais, M., Matos, M., Marques, A.C., Reis, M.A.M., Freitas, F., 2023. Preparation of porous scaffold based on poly(3-hydroxybutyrate-co-3-hydroxyvalerate-co-3-hydroxyhexanoate) and FucoPol. Polymers 15. https://doi.org/10.3390/polym15132945.

Portela-Grandío, A., Lagoa-Costa, B., Kennes, C., Veiga, M.C., 2021. Polyhydroxyalkanoates production from syngas fermentation effluents: effect of nitrogen availability. J. Environ. Chem. Eng. 9, 106662 https://doi.org/10.1016/j.jece.2021.106662.

Rangel, C., Carvalho, G., Oehmen, A., Frison, N., Lourenço, N.D., Reis, M.A.M., 2023. Polyhydroxyalkanoates production from ethanol- and lactate-rich fermentate of confectionary industry effluents. Int. J. Biol. Macromol. 229, 713–723. https://doi.org/10.1016/j.ijbiomac.2022.12.268.

Reis, M.A.M., Albuquerque, M., Villano, M., Majone, M., 2011. Mixed culture processes for polyhydroxyalkanoate production from agro-industrial surplus/wastes as feedstocks. Comprehensive Biotechnology, Second Edition, second ed. Elsevier B.V. https://doi.org/10.1016/B978-0-08-088504-9.00464-5.

Saavedra del Oso, M., Mauricio-Iglesias, M., Hospido, A., 2021. Evaluation and optimization of the environmental performance of PHA downstream processing. Chem. Eng. J. 412, 127687 https://doi.org/10.1016/j.cej.2020.127687.

Sabapathy, P.C., Devaraj, S., Meixner, K., Anburajan, P., Kathirvel, P., Ravikumar, Y., Zabed, H.M., Qi, X., 2020. Recent developments in Polyhydroxyalkanoates (PHAs) production – a review. Bioresour. Technol. 306, 123132 https://doi.org/10.1016/j.biortech.2020.123132.

Silva, F., Matos, M., Pereira, B., Ralo, C., Pequito, D., Marques, N., Carvalho, G., Reis, M.A.M., 2022. An integrated process for mixed culture production of 3-hydroxyhexanoate-rich polyhydroxyalkanoates from fruit waste. Chem. Eng. J. 427 https://doi.org/10.1016/j.cej.2021.131908.

Statistica, 2024. Statistica [WWW Document]. URL. https://www.statista.com/statistics/1010383/global-polyhydroxyalkanoate-market-size/.

United Nations Environment Programme, 2024 [WWW Document]. URL United Nations Environment Programme. https://www.unep.org/, 2.5.24.

Wang, X., Oehmen, A., Freitas, E.B., Carvalho, G., Reis, M.A.M., 2017. The link of feast-phase dissolved oxygen (DO) with substrate competition and microbial selection in PHA production. Water Res. 112, 269–278. https://doi.org/10.1016/j.watres.2017.01.064.

Yin, W., Wang, K., Xu, J., Wu, D., Zhao, C., 2018. The performance and associated mechanisms of carbon transformation (PHAs, polyhydroxyalkanoates) and nitrogen removal for landfill leachate treatment in a sequencing batch biofilm reactor (SBBR). RSC Adv. 8, 42329–42336. https://doi.org/10.1039/c8ra07839d.

Zhila, N., Shishatskaya, E., 2018. Properties of PHA bi-, ter-, and quarter-polymers containing 4-hydroxybutyrate monomer units. Int. J. Biol. Macromol. 111, 1019–1026. https://doi.org/10.1016/j.ijbiomac.2018.01.130.